

Three-micron extinction of the Titan haze in the 250–700 km altitude range: Possible evidence of a particle-aging process[★] (Research Note)

Régis Courtin¹, Sang Joon Kim², and Akiva Bar-Nun³

¹ LESIA-Observatoire de Paris, CNRS, Université Paris 06, Université Paris-Diderot, 5 place Jules Janssen, 92195 Meudon, France
e-mail: regis.courtin@obspm.fr

² School of Space Research, Kyung Hee University, 446–701 Yongin, Korea

³ Department of Geosciences, Tel-Aviv University, 69978 Tel-Aviv, Israel

Received 12 September 2014 / Accepted 27 October 2014

ABSTRACT

Context. The chemical nature of the Titan haze is poorly understood. The investigation carried out by the *Cassini-Huygens* suite of instruments is bringing new insights into this question.

Aims. This work aims at deriving the vertical variation of the spectral structure of the 3.3–3.4 μm absorption feature of the Titan haze from *Cassini* VIMS solar occultation data recorded between 250 and 700 km altitude.

Methods. We computed the transmittance of Titan's atmosphere using a spherical shell model and a radiative transfer code including the influence of CH_4 , CH_3D , and C_2H_6 , as well as the effects of absorption and scattering by the haze particles. We derived the haze extinction from a comparison of the synthetic spectra with the VIMS solar occultation spectra.

Results. We find a marked change in the relative amplitudes of the 3.33 and 3.38 μm features, which are characteristic of aromatic (double C=C chains or rings) or aliphatic (single C–C chains) structural groups, respectively. The pseudo-ratio of aromatics to aliphatics (uncorrected for the absolute band strengths) varies from 3.3 ± 1.9 at 580–700 km to 0.9 ± 0.1 at 350–450 km, and is 0.5 ± 0.1 around 250 km. The structural change from the aromatic to the aliphatic type between 580 and 480 km appears to correspond to a spontaneous aging of the particles – a transition between unannealed and hardened particles – while the further decrease of the pseudo-ratio of aromatics to aliphatics below 480 km may be related to the coating of the core particles by condensates such as heavy alkanes.

Key words. planets and satellites: individual: Titan – techniques: spectroscopic – infrared: planetary systems

1. Introduction

The exact nature of the Titan haze is currently only partly known, mainly because of limited spectroscopic observations from the ground or from space. Before the *Cassini-Huygens* era, the Titan haze particles were known to possess the following optical properties in addition to a high optical thickness in the visible range: 1) highly forward-scattering properties derived from observations by the Voyager probe (Rages et al. 1983); 2) broad near-infrared spectral features deduced from ground-based observations (Griffith et al. 1998); and 3) mid- and far-infrared spectral features observed by the Voyager IRIS spectrometer (Coustenis et al. 1999). But the chemical composition of the haze material has remained elusive, even with the help of extensive laboratory measurements carried out on simulated Titan haze material, the so-called tholins (Sagan et al. 1979; Khare et al. 1984; Coll et al. 1999; Ramirez et al. 2002; Tran et al. 2003a,b; Bernard et al. 2006; Quirico et al. 2008; Jacovi et al. 2010; Gautier et al. 2012).

After a decade of investigation by the instruments of the *Cassini-Huygens* mission, with both remote and in situ observations, the Titan haze is slowly revealing its chemical nature. New information on the optical or chemical properties of the haze have resulted from various experiments: 1) very heavy ions in the thermosphere (900–1100 km) were detected by the Ion and

Neutral Mass Spectrometer (INMS; Waite et al. 2007); 2) refractory organics were isolated in the cores of the haze particles collected by the Aerosol Collector and Pyrolyser (ACP) at low altitude (20–130 km; Israël et al. 2005); 3) the scattering properties and the optical thickness of the haze between 480 and 1600 nm were derived from low-altitude data ($z < 150$ km) obtained by the Descent Imager/Spectral Radiometer (DISR; Tomasko et al. 2008); 4) spectral features were observed at 3.2–3.6 μm in solar occultation data obtained by the Visual Infrared Mapping Spectrometer (VIMS; Bellucci et al. 2009) as well as a feature at 2.3 μm , all of which were attributed to absorption by mostly heavy alkanes (or alkane particles) with an enhancement of these alkane features between 127 and 300 km (Kim et al. 2011; Sim et al. 2013; Kim & Courtin 2013); 5) the mid- and far-infrared spectral properties were retrieved from measurements by the Composite Infrared Spectrometer (CIRS; Anderson & Samuelson 2011; Vinatier et al. 2012); and 6) the 3.3- μm feature characteristic of polycyclic aromatic hydrocarbons (PAHs) was detected from VIMS observations through high-altitude atmospheric layers (600–1250 km; Dinelli et al. 2013; López-Puertas et al. 2013).

These *Cassini-Huygens* results outline the general picture of the haze chemical composition in Titan's atmosphere as follows: in the 600–1250 km altitude range, the haze material appears to be composed of heavy organics such as PAHs; from 600 to 300 km, PAHs and heavy alkanes (or alkane particles) seem to co-exist within a mantle, but the concentration of the former component progressively weakens so that the latter becomes

[★] VIMS transmission spectra data are only available at the CDS via anonymous ftp to cdsarc.u-strasbg.fr (130.79.128.5) or via <http://cdsarc.u-strasbg.fr/viz-bin/qcat?J/A+A/573/A21>

dominant below 300 km, down to at least 127 km. The core material itself, composed of refractory organics, appears to be preserved down to the surface.

On the other hand, theoretical modeling of the physico-chemical processes that lead to the formation of the haze particles in Titan's upper atmosphere provides another avenue for deciphering their nature (Podolak et al. 1984; Bar-Nun et al. 1988; Dimitrov & Bar-Nun 1999). In particular, Dimitrov & Bar-Nun (1999) proposed a model of an energy-dependent agglomeration of hydrocarbon aerosol particles in Titan's atmosphere, and several of the particle properties predicted by their model have been confirmed by the DISR results (Bar-Nun et al. 2008). On that basis, Dimitrov & Bar-Nun (2002, 2003) investigated the possible aging or hardening of the haze particles and proposed that there might be a region of major change in the haze properties around 570 or 620 km altitude, depending on the type of aging, either spontaneous or forced: above this level, the haze particles are fine and sticky, containing a large proportion of double-bond C=C; below this, the particles become less sticky and completely aged or hardened, with a smaller proportion of double bonds.

Among several haze absorption features present in the 2–5 μm interval of the VIMS solar occultation data, the feature at 3 μm is the most prominent and is the highest vertically resolved feature. Its structure can be derived up to 700 km. Previously, only a limited selection of haze spectra derived from the VIMS data around 3 μm have been presented (Kim et al. 2011; Kim & Courtin 2013; Sim et al. 2013). In this work, we take full advantage of the VIMS solar occultation data of Bellucci (2008), and we examine the vertical variation of the 3- μm feature to verify or confute the transition proposed by Dimitrov & Bar-Nun (2002, 2003). We then discuss an updated scenario for the aging of the haze particles, based on the so-derived variations of the chemical composition of the haze.

2. Vertically resolved extinction around 3 μm

The detailed description of the VIMS solar occultation experiment has been given by Bellucci (2008) and Bellucci et al. (2009). The VIMS instrument consists of 256 infrared spectral channels covering the interval 0.85 to 5.1 μm with a spectral resolution of 0.016 μm (Brown et al. 2004). The field of view of the VIMS instrument is 6 \times 6 mrad, and each spectro-image covers a portion of the atmosphere 50–60 km in size when observed at 8000–10 000 km from Titan. The observations were carried out on January 15, 2006, during solar egress at 71°S, and the size of the solar disk was about 7 to 10 km in the VIMS field of view. The noise level was estimated to be 7.5×10^{-3} in terms of transmittance between 3.0 and 3.8 μm . The VIMS spectra are presented in Fig. 1, along with the $\pm 2\sigma$ noise level.

Analyzing the same VIMS data between 127 and 300 km, Kim et al. (2011) previously found that the optical-depth (τ) spectra of the haze are very similar to each other, indicating nearly homogeneous chemical properties in this altitude range; they also found an enhancement of the 3.33- μm feature near or below 127 km and above 300 km. Here, we mainly focus on high-altitude data (250–700 km) in which the transition region proposed by Dimitrov & Bar-Nun (2002, 2003) may occur.

We adopted the same radiative transfer analysis as was used in our previous works (Kim et al. 2011, 2012, 2014; Kim & Courtin 2013; Sim et al. 2013), assuming a spherically homogeneous shell model. The temperature profile and the CH₄ vertical distribution are the same as were used by Sim et al. (2013) and Kim & Courtin (2013). In synthesizing the VIMS spectra, we

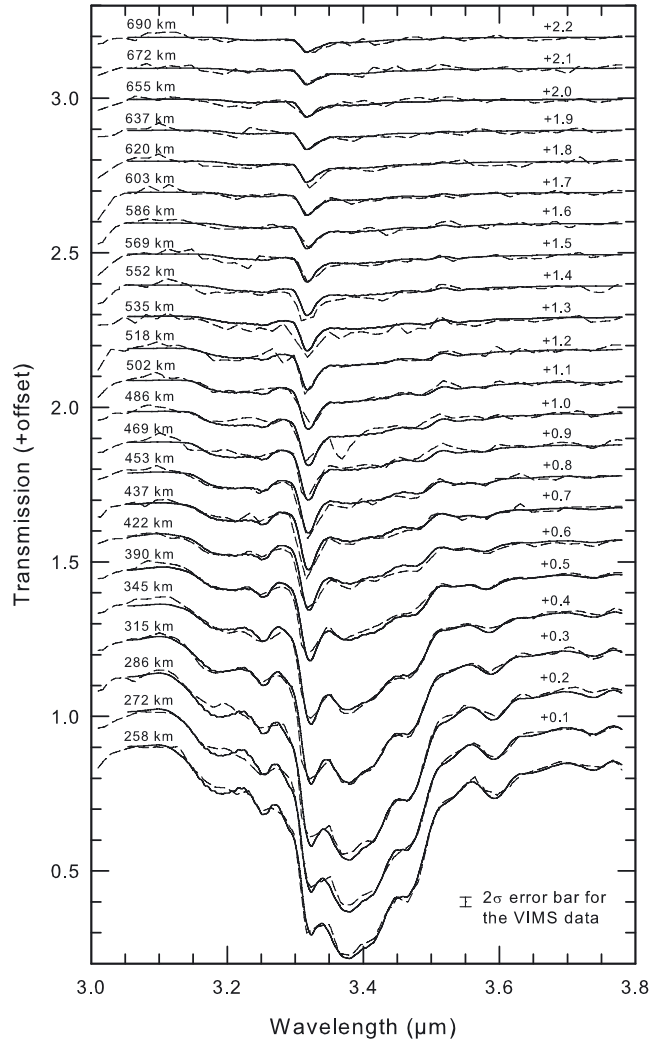


Fig. 1. Comparison between synthetic spectra (solid lines) and VIMS spectra (dashed lines) in the 3.0–3.8 μm interval for the 250–700 km altitude range. For clarity, offsets are introduced as indicated. The $\pm 2\sigma$ error bars for the VIMS spectra are adopted from previous estimates (Bellucci et al. 2009).

used the HITRAN2012 database (Rothman et al. 2009) for the line-by-line parameters of the 3- μm bands of ¹²CH₄, ¹³CH₄, and CH₃D. The influence of the ν_7 band of C₂H₆ was also included, adopting the same model as was used by Kim et al. (2011). The radiative and collisional excitation and de-excitation of CH₄, as well as the effects of anisotropic scattering by the haze particles, were taken into account as detailed by Kim et al. (2012, 2014), and Sim et al. (2013).

In Fig. 1, we compare the model spectra with the VIMS data recorded between 250 and 700 km. The overall fit is satisfactory, although there is a notable discrepancy at 3.37 μm for the spectrum at 486 km altitude. This is due to a conspicuous absorption feature in the VIMS data that cannot be reproduced by our model. If an inhomogeneous region exists within one of the shells, it cannot be reproduced by the model because we assumed spherically homogeneous shells to represent Titan's atmosphere. Another possibility is an artifact in the spectrum recorded at 486 km since the transmission spectra at 469 and 502 km do not show any hint of this absorption feature. Between 3.05 and 3.15 μm , certain VIMS spectra exhibit transmissions greater than unity. Although the transmission spectra are only directly influenced by the projected size of the Sun on the limb

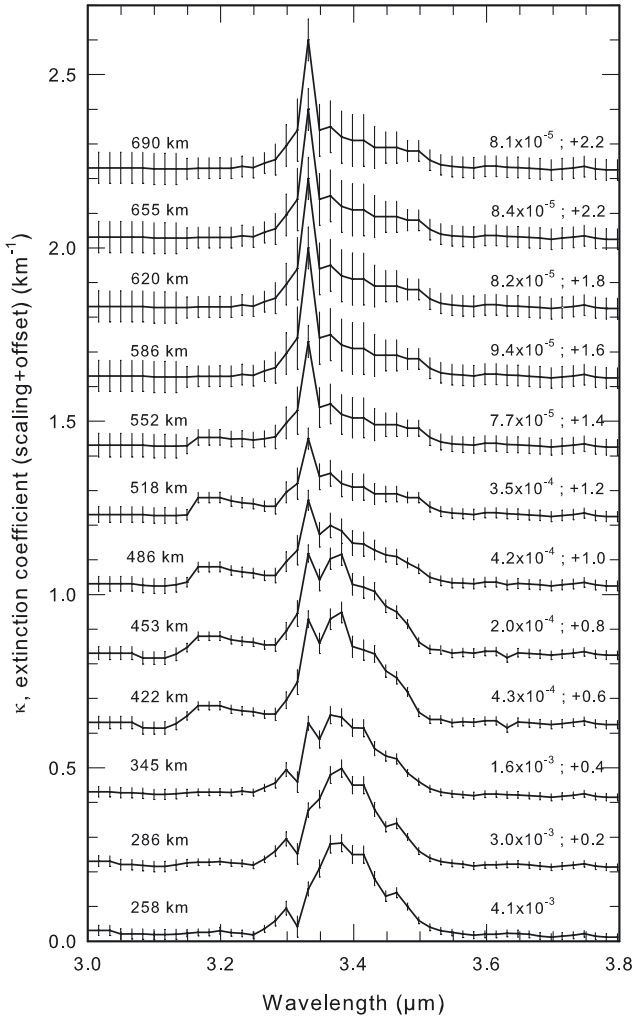


Fig. 2. Spectral variation of the extinction coefficients derived from the fits shown in Fig. 1. Scaling factors are applied as indicated to make the comparison between different altitudes more meaningful. For clarity, only half of the coefficients are displayed, and offsets are introduced as indicated. The $\pm 1\sigma$ error bars are shown.

(about 1 mrad), scattered light may enter the VIMS field of view from other directions than the direct line of sight. Similar abnormally high transmissions were reported at $2.02 \mu\text{m}$ for the 400–500 km altitude range by Bellucci et al. (2009); these authors suggested possible forward scattering by the detached haze layer (DHL) within the field of view, while the Sun was observed through the clear gap.

For clarity, we present in Fig. 2 only half of the extinction coefficients, $\kappa(\lambda) = \tau(\lambda)/\delta z$, derived from the fits shown in Fig. 1. The $\pm 1\sigma$ error bars are estimated from the VIMS error bars as well as uncertainties in the radiative transfer model. Above the 690 km level, the absorption features are too weak to derive meaningful extinction coefficients.

Two main absorption peaks appear in the τ -spectra, one at $3.33 \mu\text{m}$ and a broader one at 3.37 – $3.40 \mu\text{m}$, and their relative amplitudes vary quite significantly between 700 and 250 km. These absorptions are characteristic of two structural groups of organic molecules. In the 3.25 – $3.35 \mu\text{m}$ interval, aromatic bands arise from three main functional groups: olefinic CH_2 (asymmetric), olefinic CH , and olefinic CH_2 (symmetric), while in the 3.35 – $3.50 \mu\text{m}$ interval, aliphatic bands are due to the following groups: aliphatic CH_3 (asymmetric), aliphatic CH_2 (asymmetric), tertiary CH , aliphatic CH_3 (symmetric), and aliphatic

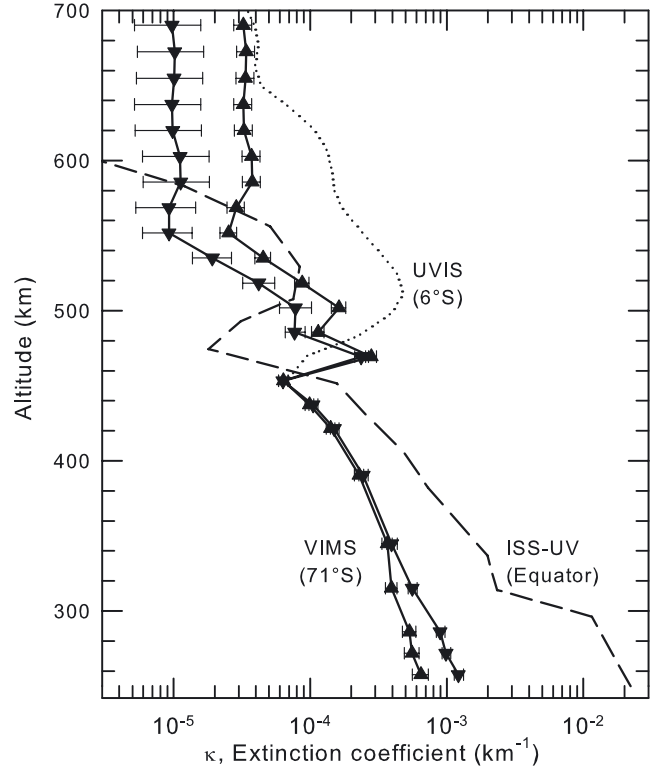


Fig. 3. Variation between 250 and 700 km of the haze extinction coefficients at $3.33 \mu\text{m}$ (solid line with upward triangles for the aromatic component) and $3.38 \mu\text{m}$ (solid line with downward triangles for the aliphatic component). The extinction coefficient profiles inferred by West et al. (2011) from ISS/UV imaging (dashed line) and by Koskinen et al. (2011) from UVIS stellar occultation measurements (dotted line) are also represented. The local maxima around 500 km correspond to the detached haze layer.

CH_2 (symmetric; Cruikshank et al. 2014). From the spectra shown in Fig. 2, we extracted the vertical profiles of the haze extinction coefficient $\kappa(\lambda)$ at two wavelengths, $\lambda_1 = 3.33 \mu\text{m}$ and $\lambda_2 = 3.38 \mu\text{m}$, representative of the aromatic and aliphatic components in the haze composition. They are shown in Fig. 3. In addition to the steady increase of the extinction coefficient from 700 to 250 km altitude, an obvious feature of both profiles is the local maximum at 470 km, with a broad feature between 450 and 530 km, which corresponds to the DHL. In this respect, it is worth comparing these profiles with that derived by West et al. (2011) from images recorded by the Cassini Imaging Sub-System (ISS) in the UV ($\lambda_{\text{eff}} = 343 \text{ nm}$) in May 2006, and by Koskinen et al. (2011) from stellar occultation observations made by the Cassini Ultra-Violet Imaging Spectrograph (UVIS) in February 2008 (see Fig. 3). In these profiles, which correspond to equatorial and 6°S latitudes, respectively, the local maximum is at 500–510 km. This is 30–40 km higher than the maximum in the VIMS profiles. Incidentally, West et al. showed that the altitude of the maximum brightness of the DHL decreased from $\sim 500 \text{ km}$ to $\sim 320 \text{ km}$ during the period 2007–2010, roughly centered on the equinox. Since the VIMS data were acquired about four months before the ISS images, the location of the DHL should be roughly the same. On the other hand, West et al. also showed that the altitude of the peak brightness depends on latitude, with the difference between equatorial and polar altitudes on the order of 10 km (June 2005) to 30 km (August 2009). The fact that the VIMS data were obtained at a latitude of 71°S partly explains the observed altitude

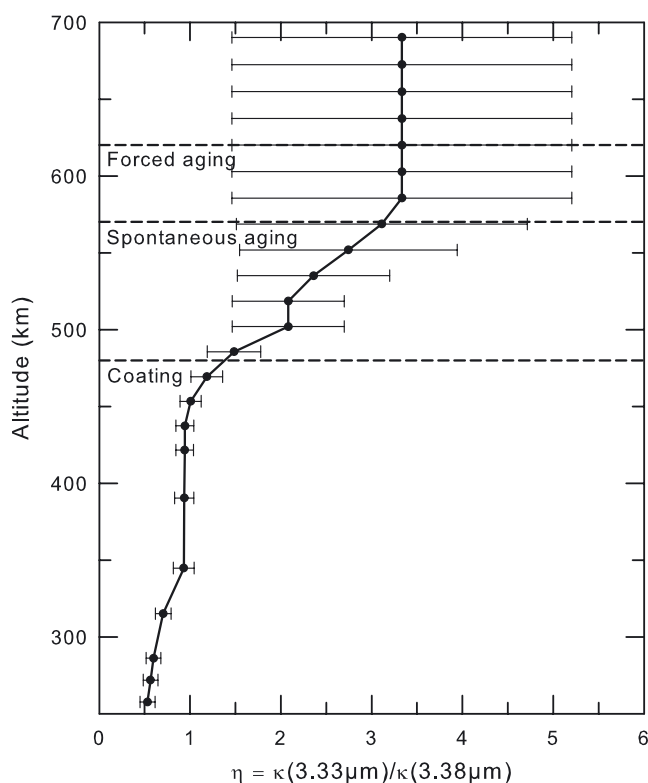


Fig. 4. Vertical variation of the ratio between the extinction coefficients at 3.33 and 3.38 μm , which is proportional to the ratio between the aromatic and aliphatic components in the haze material. The altitude limits correspond to the onset of the forced aging, spontaneous aging and coating processes.

difference. Furthermore, we caution that the determination of the altitude of the DHL in the VIMS profile may be somewhat biased by the potential artifact already noted in the transmission spectrum at 486 km. The unexplained remnant of the altitude difference, on the order of 20 km, may be due to such a bias.

Figure 4 presents the vertical profile of the ratio $\eta = \kappa(\lambda_1)/\kappa(\lambda_2)$ between the extinction coefficients shown in Fig. 3. This ratio can only be considered as a pseudo-ratio of aromatics to aliphatics characteristic of the haze material because it is not corrected for the absolute strengths of the absorption bands involved (a detailed model of all these bands is not possible at this point). The profile exhibits a steady decrease from 700 km to 250 km, where four main regions can be distinguished: a) the profile is roughly constant in the 580–700 km range with a value of 3.3 ± 1.9 ; b) there is a steep decrease with a slope on the order of -0.018 km^{-1} in the 450–580 km range; c) the profile is again roughly constant with a value of 0.9 ± 0.1 in the 350–450 km range; and d) there is another decrease with a shallower slope of -0.005 km^{-1} below 350 km. We discuss below the connection between the vertical variation of the absorption properties of the haze and the aging and hardening process proposed by Dimitrov & Bar-Nun (2002, 2003).

3. Discussion

A thorough investigation of the chemical composition of Titan's mid-atmospheric aerosols produced by photochemical processes (Jacovi et al. 2010; Dimitrov & Bar-Nun 2003) has shown that in the solid phase, the material has aromatic rings that have conjugated double bonds: biphenyl, naphthalene, phenyl acetylene, and condensed rings. Another large proportion consists

of polyvinyls $\text{H}_2\text{C} = \text{CH}-(\text{CH}=\text{CH})_n-\text{CH}=\text{CH}_2$ that again have conjugated double bonds like in aromatics, and N-mixed hydrocarbons. These polymers have regularly alternating (i.e., conjugated) double or single and triple or single bonds, which open either spontaneously (spontaneous aging; Dimitrov & Bar-Nun 2002), or under the action of some external factors (forced aging; Dimitrov & Bar-Nun 2003). This is called cross-linking, which produces a three-dimensional matrix insoluble in any solvent and removable only by burning in pure oxygen. The forced aging stems from very diverse processes such as charging, photolysis, radiolysis, thermolysis, and chemical effect of environment. The main distinction between spontaneous and any forced aging is that, while both possess the same thermodynamics, they have different kinetics, the forced aging being faster and proceeding in different pathways than the spontaneous aging.

The comparison of the aging rate and sedimentation and growth rates of the particles shows that the Titan haze layers can be divided into two subdomains. The upper subdomain contains a small portion (<5%) of the total aerosol bulk, with unannealed aerosol particles being fine and sticky. The lower subdomain contains the main portion (>95%) of the aerosol bulk, which consists of completely aged, coarsely dispersed particles. The borderline between these subdomains has been established at around 570 km for spontaneous aging (Dimitrov & Bar-Nun 2002) and around 620 km for forced aging (Dimitrov & Bar-Nun 2003). Thus, while the haze particles are descending through the atmosphere, the real aromatic rings remain the same, but the polyvinyls lose many of the double bonds by opening them to form bonds between adjacent chains. While the aromatic rings remain the same, the polyvinyls lose their aromatic-like structure by cross-linking (Jacovi et al. 2010; Dimitrov & Bar-Nun 2003). Another process occurs around 480 km and below: the coating of the aerosols by the available aliphatic condensable gases in the atmosphere such as methane, ethane, propane, and heavier alkanes (Dimitrov & Bar-Nun 1999). Some ethylene, acetylene, and nitriles are also present, but far fewer than methane and ethane. All this means that as we move down in Titan's atmosphere, we should see less aromatics and more aliphatics, as the VIMS spectra show.

In Fig. 4, we compare the vertical profile of the pseudo-ratio of aromatics to aliphatics, η , with these predictions for the aging and coating processes that affect the haze material. The altitudes are indicated at which the forced aging (620 km) and spontaneous aging (570 km) processes as well as the coating (480 km) process become effective. The limit for the onset of spontaneous aging agrees best with the lower boundary of the uppermost region described in the previous section (570 vs. 580 km), where $\eta \sim 3$. Given the large error bars that affect the values of η in the 580–700 km range, however, it is difficult to distinguish between the influences of the forced and spontaneous aging processes. The combined effects of these two processes appear to be confirmed by the steep decrease of η below 580 km, however. Furthermore, the limit of the coating process is quite close to the lower boundary of the region characterized by a steep decrease (480 vs. 470 km). Thus, coating of the haze particles by condensable aliphatics such as heavy alkanes, as described by Dimitrov & Bar-Nun (1999), may explain the further decrease of η from 480 to 450 km, and also between 350 and 250 km.

4. Conclusions

We have derived the vertical variation of the spectral structure of the 3.3–3.4 μm absorption feature of the Titan haze from VIMS solar occultation data recorded between 250 and 700 km

altitude. We found a marked change in the relative strengths of the 3.33 and 3.38 μm absorption peaks, which are characteristic of the aromatic (double C=C bonds or rings) and aliphatic (single C–C bonds) components of the haze material composition. The pseudo-ratio of aromatics to aliphatics, which is uncorrected for the absolute band strengths, varies from 3.3 ± 1.9 at 580–700 km to 0.9 ± 0.1 at 350–450 km and 0.5 ± 0.1 around 250 km. The steep decrease of this ratio between 580 and 480 km, indicating a change from aromatic to aliphatic composition, appears to be caused by the combined effects of spontaneous and forced aging of the haze particles, that is, by a transition between unannealed and hardened particles, as proposed by Dimitrov & Bar-Nun (2002, 2003), while its further decrease below 480 km may be related to the coating of the core particles by condensates such as heavy alkanes, as described by Dimitrov & Bar-Nun (1999).

Acknowledgements. S.J.K. acknowledges support from the Brain Korea 21 Plus (BK21+) program through the National Research Foundation of Korea funded by the Ministry of Education, Science and Technology, and from the Korean Astronomy and Space Science Institute.

References

- Anderson, C. M., & Samuelson, R. E. 2011, *Icarus*, 212, 762
 Bar-Nun, A., Kleinfeld, I., & Ganor, E. 1988, *J. Geophys. Res.*, 93, 8383
 Bar-Nun, A., Dimitrov, V., & Tomasko, M. 2008, *Planet. Space Sci.*, 56, 708
 Bellucci, A. 2008, Ph.D. Thesis, Université Pierre et Marie Curie, Paris, France
 Bellucci, A., Sicardy, B., Drossart, P., et al. 2009, *Icarus*, 201, 198
 Bernard, J.-M., Quirico, E., Brissaud, O., et al. 2006, *Icarus*, 185, 301
 Brown, R. H., Baines, K. H., Bellucci, G., et al. 2004, *Space Sci. Rev.*, 115, 111
 Coll, P., Coscia, D., Smith, N., et al. 1999, *Planet. Space Sci.*, 47, 1331
 Coustenis, A., Schmitt, B., Khanna, R. K., & Trotta, F. 1999, *Planet. Space Sci.*, 47, 1305
 Cruikshank, D. P., Dalle Ore, C. M., Clark, R. N., & Pendleton, Y. J. 2014, *Icarus*, 233, 306
 Dimitrov, V., & Bar-Nun, A. 1999, *J. Aerosol Sci.*, 30, 35
 Dimitrov, V., & Bar-Nun, A. 2002, *Icarus*, 156, 530
 Dimitrov, V., & Bar-Nun, A. 2003, *Icarus*, 166, 440
 Dinelli, B. M., López-Puertas, M., Adriani, A. et al. 2013, *Geophys. Res. Lett.*, 40, 1489
 Gautier, T., Carrasco, N., Mahjoub, A. et al. 2012, *Icarus*, 221, 320
 Griffith, C. A., Owen, T., Miller, G. A., & Geballe, T. 1998, *Nature*, 395, 575
 Israël, G., Szopa, C., Raulin, F. et al. 2005, *Nature*, 438, 796
 Jacovi, R., Laufer, D., Dimitrov, V., & Bar-Nun, A. 2010, *J. Geophys. Res.*, 115, E07006
 Khare, B. N., Sagan, C., Arakawa, E. T., et al. 1984, *Icarus*, 60, 127
 Kim, S. J., & Courtin, R. 2013, *A&A*, 557, L6
 Kim, S. J., Jung, A., Sim, C. K., et al. 2011, *Planet. Space Sci.*, 59, 699
 Kim, S. J., Sim, C. K., Lee, D. W., et al. 2012, *Planet. Space Sci.*, 65, 122
 Kim, S. J., Sim, C. K., Sohn, M. R., & Moses, J. I. 2014, *Icarus*, 237, 42
 Koskinen, T. T., Yelle, R. V., Snowden, D. S., et al. 2011, *Icarus*, 216, 507
 López-Puertas, M., Dinelli, B. M., Adriani, A. et al. 2013, *ApJ*, 770, 132
 Podolak, M., Bar-Nun, A., Noy, N., & Giver, L. 1984, *Icarus*, 57, 72
 Quirico, E., Bernard, J.-M., Schmitt, B., et al. 2008, *Icarus*, 198, 218
 Rages, K., Pollack, J. B., & Smith, P. H. 1983, *J. Geophys. Res.*, 88, 8721
 Ramirez, S. I., Coll, P., Da Silva, A., et al. 2002, *Icarus*, 156, 515
 Rothman, L. S., Gordon, I. E., Barbe, A., et al. 2009, *J. Quant. Spectr. Rad. Transf.*, 110, 533
 Sagan, C., & Khare, B. N. 1979, *Nature*, 277, 102
 Seo, H., Kim, S. J., Kim, J. H., et al. 2009, *Icarus*, 199, 449
 Sim, C. K., Kim, S. J., Courtin, R., et al. 2013, *Planet. Space Sci.*, 88, 93
 Tomasko, M. G., Doose, L., Engel, S., et al. 2008, *Planet. Space Sci.*, 56, 669
 Tran, B. N., Ferris, J. P., & Chera, J. J. 2003a, *Icarus*, 162, 114
 Tran, B. N., Joseph, J. C., Ferris, J. P., et al. 2003b, *Icarus*, 165, 379
 Vinatier, S., Rannou, P., Anderson, C. M., et al. 2012, *Icarus*, 219, 5
 Waite Jr., J. H., Young, D. T., Cravens, T. E., et al. 2007, *Science*, 316, 870
 West, R. A., Balloch, J., Dumont, P., et al. 2011, *Geophys. Res. Lett.*, 38, L06204